AMER. ZOOL., 38:743–754 (1998)

Post-Activation Potentiation—A Clue for Simplifying Models of Muscle Dynamics[1]

IAN E. BROWN AND GERALD E. LOEB[2]

MRC Group in Sensory-Motor Neuroscience and the Department of Physiology, Queen's University, Kingston, Ontario, K7L 3N6, Canada

SYNOPSIS. Post-activation potentiation is a phenomena that occurs only in fast-twitch muscle fibers. Its main effect is to enhance muscle force at sub-maximal activation levels for a short duration of time following previous muscle activation. We characterized this phenomenon in feline caudofemoralis (CF) muscle (composed of 100% fast-twitch muscle fibers) to understand its importance during physiological patterns of activation. During such patterns (*e.g.*, 43 pps, 8 pulse trains delivered at 1 sec intervals) CF potentiated rapidly and apparently maximally. When CF was allowed to relax, potentiation decayed slowly with a time constant 20–40× slower than the rise-time. The level of potentiation reached during the potentiating paradigm was stable in response to a wide range of stimuli, including various stimulation rates (15–120 pps) and various inter-train intervals (up to 10 sec). The shape of the twitch force-length curve for potentiated CF was similar to that of the tetanic force-length curve in either the potentiated or unpotentiated state. In contrast, the shape of the twitch force-length curve for unpotentiated CF was shifted markedly to the right accompanied by a narrowing of the curve's peak. We conclude from our observations that fast-twitch muscle fibers operate and should be modeled in a state of full potentiation, and that modeling the potentiated state may actually be simpler than modeling the unpotentiated state.

INTRODUCTION

Studies of the neural control of movement generally tend to ignore muscle and its properties, but recent work has suggested that the intrinsic properties of muscle may have large effects on the control problem (Loeb *et al.*, 1994; Brown and Loeb, 1998). If we accept the notion that various motor control strategies may be designed specifically to take advantage of key muscle properties, then we need accurate models of those properties to understand such strategies. Accurate models of muscle do exist for the special case of maximal activation (*e.g.*, Brown *et al.*, 1996*b*), but unfortunately we still lack an adequate understanding of muscle properties during physiological patterns of activation.

The mathematical transfer from neural activation to muscle force shown in Figure 1A reflects a common design for models of muscle (Zajac, 1989; Brown *et al.*, 1996*b*). Force is presumed to be the product of three independent factors: F_{ACT}, FL and FV. F_{ACT} is a measure of muscle activation that depends on neural activation 'u(t)'. FL is the isometric force-length relation (dependent upon length) and FV is the force-velocity relation (dependent upon velocity). This basic design assumes independence between these three functions. In principle, any one of these functions can be characterized by holding the other two functions constant at any value. However, this presumed independence needs to be tested to ensure that the model is accurate, particularly over the range of input conditions of u(t), L and V for which the model will be applied.

Recently, Scott *et al.* (1996) examined the question of independence between the FL and FV relationships while holding F_{ACT} constant at maximal activation. Their results showed that by choosing carefully an appropriate FL curve based on the structure of the sarcomere, they could indeed demonstrate independence between the FL and

[1] From the symposium *Muscle Properties and Organismal Function: Shifting Paradigms* presented at the Annual Meeting of the Society for Integrative and Comparative Biology, 26–30 December 1996, at Albuquerque, New Mexico.

[2] E-mail: loeb@biomed.queensu.ca

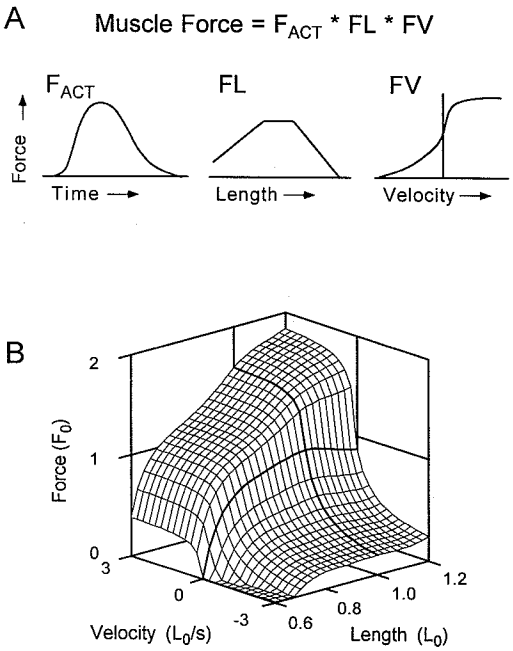

FIG. 1. **A.** Muscle force is assumed to be the product of three independent functions: F_{ACT}, FL and FV. Typical examples of what these three functions look like are plotted here. **B.** The Force-Length-Velocity surface for maximally activated feline soleus muscle including both active and passive force (adapted from Brown *et al.*, 1996*b*).

FV relationships for shortening velocities. However, they discovered that the FL and FV relationships were not independent for lengthening velocities. This observation resulted in the mathematical formulation being changed somewhat with FV becoming dependent upon length as well as velocity. The force-length-velocity surface based upon Scott *et al.*'s data is shown in Figure 1B.

The next step in the design of the muscle model is to examine more closely the proposed independence of F_{ACT} and FL; previous modeling and experimental studies have suggested that F_{ACT} is not independent of FL and FV (Rack and Westbury, 1969; Stephenson and Wendt, 1984; Shue *et al.*, 1995). We have chosen to test this independence with the feline muscle caudofemoralis (CF), a hip extensor/abductor that originates with almost no tendon from the transverse processes of the second and third caudal vertebrae and inserts with a long tendon into the patellar fascial complex. We chose CF because it possesses a unique combination of three characteristics that simplify the collection and interpretation of experimental data (Brown *et al.*, 1998): a homogeneous parallel-fibered architecture, very short aponeuroses permitting an experimental setup with minimal in-series elasticity, and a homogeneous fiber-type population. The difficulty with this preparation is that the homogeneous fiber population is of the fast-twitch variety. Fast-twitch muscles demonstrate a complex phenomenon not found in slow-twitch muscles known as post-activation potentiation (PAP, Manning and Stull, 1982; Moore and Stull, 1984), in which recent activation of a muscle significantly increases the force produced by subsequent sub-maximal activation.

An important consequence of PAP affecting force production is that F_{ACT} needs to account for the increased force observed during PAP. Furthermore, there is evidence that PAP may affect the FV relation (Grange *et al.*, 1995) as well as the F_{ACT}-FL interdependence (Close, 1972; Moore and Persechini, 1990) within the physiological range of motion for many muscles, including CF (Brown *et al.*, 1996*a*; Brown *et al.*, 1998). If the mathematical design of F_{ACT} is based upon the unpotentiated state, then various corrective terms will have to be added to account for the changes induced by PAP. If instead the normal operating state of muscle is the potentiated state, and if a model is based upon that state, then potentially complex corrective terms would be unnecessary. This second alternative and its potential benefits are considered here from a variety of perspectives including experimental design, model design and physiological relevance.

METHODS

The experimental apparatus used in this study is similar to one used and described previously for feline soleus muscle (Scott *et al.*, 1996). All experiments were carried out in cats of either sex (2.4–5.1 kg) under deep anesthesia (sodium pentobarbital) as determined by the absence of pedal withdrawal. Briefly, the feline CF muscle was studied *in situ*, dissected free of surround-

ing tissue with its origin, innervation and blood supply left intact. The length of the muscle fascicles was controlled by clamping onto caudal vertebrae Ca2 and Ca3 (CF origin) and on to the insertion tendon just at the point where the last fibers terminate, eliminating virtually all series-compliance in the linkage. The insertion clamp was attached to a computer-controlled muscle puller to carefully establish specific muscle lengths. Isometric force output at each discrete muscle length was obtained from a force transducer in-series with the muscle puller. Electrical stimulation was monitored by recording M-waves via two multistranded stainless steel wire electrodes inserted transversely through the muscle approximately 5 mm apart. Computer templates controlled the length and stimulus patterns simultaneously for long preprogrammed sequences defining entire experimental protocols in 1.667 ms steps. During each step, the computer program recorded values for both the force and a rectified, bin-integrated representation of the M-waves. Force data were digitally filtered after the experiment using a double-pass, second-order Butterworth filter with a 3 dB cutoff frequency of 120 Hz.

Electrical stimulation was applied to the ipsilateral L7 and S1 ventral roots by platinum-iridium hook electrodes in a paraffin oil pool, after ascertaining that these were the only roots providing efferent innervation to CF. To expose these roots, an L5 to S1 laminectomy was performed and the corresponding dorsal roots ligated and retracted to reveal the ventral roots. To avoid stimulation of the other muscles of the leg, the femoral, obturator, distal sciatic and gluteus maximus nerves were all ligated. A pool was created with skin flaps around both the muscle and exposed spinal cord and filled with paraffin oil. Both the pool and the animal's core temperature were maintained thermostatically at 37°C ± 1°. The muscle and nerve preparation were allowed to equilibrate for at least 1 hr prior to data collection.

At the beginning of each experiment a tetanic FL curve was collected in the unpotentiated state (as described below). Preliminary estimation of L_0 was made based upon *in situ* anatomical lengths (Brown *et al.,* 1998). Based on this estimate, isometric tetanic contractions (120 pps, 12–15 p trains) were elicited at 0.7, 0.8, 0.9, 0.95, 1.0, 1.05, 1.1 and 1.2 L_0. The "true" L_0 was then chosen as the length at which maximal tetanic isometric force (F_0) could be elicited.

Two basic protocols of stimulation were used in this study to produce two different states of muscle: unpotentiated and potentiated. Data in the unpotentiated state were collected prior to data in the potentiated state. For the unpotentiated protocols, all stimuli were separated by 5 minute intervals to avoid potentiation. The potentiated protocols used stimuli separated by 1–10 sec. For the potentiated protocols, the muscle and nerve preparation was allowed to equilibrate for 1 hr between each protocol. Because of previous evidence that the length at which a potentiating stimulus occurs can affect the subsequent level of potentiation (Moore and Persechini, 1990), potentiating stimuli were given at either three different lengths (0.75, 0.95 and 1.15 L_0) or at five different lengths (0.75, 0.85, 0.95, 1.05 and 1.15 L_0) to cover the physiological range of motion for CF (Brown *et al.,* 1996*a*; Brown *et al.,* 1998). The lengths were sequenced from shortest to longest and then repeated. In all paradigms stimulation voltage (0.2 ms rectangular wave pulses) was five times higher than the threshold required to elicit an M-wave. M-wave activity was monitored continuously to ensure complete activation of the entire muscle throughout the experiment. Force potentiation was determined with one of two indices. Initial experiments were limited by software so that all stimuli in a single paradigm had to have the same periodic interval. Therefore, in these initial experiments a measure of potentiation was obtained every 6th or 7th train by inserting a standard train of 5 pulses at 30 pps while holding the muscle isometric at 1.0 L_0 and measuring the peak force. Improved software in the later experiments permitted insertion of single isometric twitches at 1.0 L_0 one second before specified experimental trains so that peak twitch force could be used as a measure of potentiation.

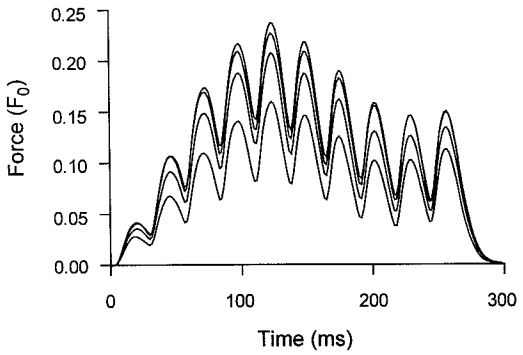

FIG. 2. Force traces from an experimental protocol of 37.5 ppsec, 10 p trains at 2 min intervals (at a length of 1.0 L_0). The first train produced the least force with subsequent trains producing progressively larger forces. Force is represented in units of F_0—maximal tetanic isometric force. (These data from CF62; similar results from CF26.)

RESULTS

The first series of experiments used trains of 10 pulses (p) at a physiological frequency of 37.5 pulses per second (pps) but an unphysiological interval of 2 min between trains, with no additional stimuli to measure potentiation. This produced a steady increase in force output from one train to the next, as shown in Figure 2. This simple paradigm demonstrates clearly that the unpotentiated state cannot be the normal physiological state as it is impossible to remain in that state for more than one contraction, even at these long intervals between successive stimuli. It was observed that five minute intervals were required between successive stimuli to ensure no significant potentiation effects (not shown).

The purpose of the second series of experiments was to determine how to collect a reasonable amount of data without inducing fatigue in the fast-twitch, fatiguable fibers comprising the CF muscle. Preliminary results (not shown) suggested that shorter intervals (*e.g.,* 1 sec) between stimuli tended to fatigue CF faster than longer intervals. Using 10 p trains at 60 pps, we examined three different stimulus intervals (4, 7 and 10 sec) to determine if we could avoid fatigue, while at the same time develop the same level of potentiation as might be expected under more physiological conditions of short stimulus intervals. The level of potentiation for each of these paradigms is shown in Figure 3A as a function of stimulus train number. The associated force profiles from the 4 sec interval paradigm are shown in Figure 3B. The preparation was allowed to equilibrate for 1 hr between each of the three paradigms. The potentiating effect of successive trains was the same for inter-train intervals of 4 and 7 sec but declined when the interval reached 10 seconds, suggesting that intervals of 7 sec duration or less produce equivalent levels of potentiation (note that the 10 sec paradigm was run before the 4 and 7 sec paradigms, so fatigue was not a factor.) We therefore chose 7 sec as the optimal interval for reaching and maintaining potentiation while avoiding fatigue.

The third series of experiments were designed to study a wider range of stimulus frequencies and train intervals such as might occur during cyclical behaviors such as locomotion. Two paradigms were developed to test the hypothesis that the level of potentiation that occurs under physiological conditions of recruitment rapidly saturates and tends to remain at a stable value. Because no data are available on the firing frequencies of motor units in CF, we assumed that the firing frequencies typical of other fast-twitch motor units would be appropriate for use with CF (*i.e.,* 15–60 pps, burst duration of 150–300 ms, Bigland and Lippold, 1954; Bellemare *et al.,* 1983; Hoffer *et al.,* 1987). The first paradigm used 60 pps, 10 p trains at 7 sec intervals to potentiate the muscle (Fig. 4). The stimulus frequency was then varied between 15 and 60 pps while maintaining constant both the number of pulses (8) and the inter-stimulus interval (7 sec). We then examined the effects on potentiation of an unphysiological tetanic stimulus (120 pps. 12 p trains) while maintaining the 7 sec interval. The level of potentiation during this paradigm never varied by more than 5% as can be seen in Figure 4.

The second paradigm in this series used a more physiological pattern of activation to reach steady-state potentiation that was developed from the first series—43 pps 8p trains at 1 sec intervals, similar to the recruitment of CF in brief bursts during tread-

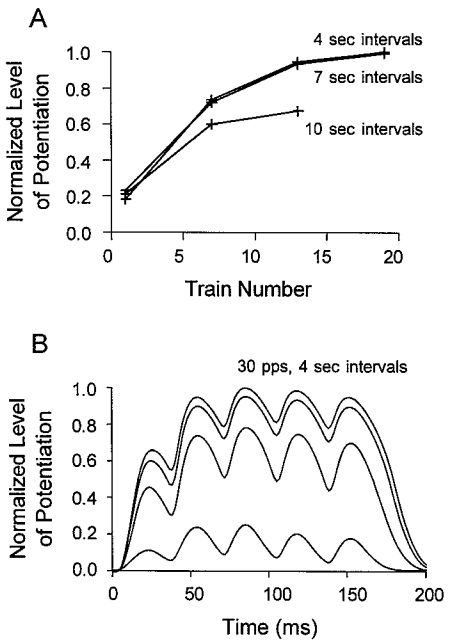

FIG. 3. Data from initial experiments when the level of potentiation was measured through peak force of a 30 pps 5p train at 1.0 L_0. **A.** Each data point represents the peak force from one of these trains. Data were normalized to the maximal peak force measured during this experiment from a 30 pps 5p train at 1.0 L_0. Intervening potentiating stimuli were 60 pps, 10p trains at three sequential muscle lengths as described in the methods (force data from these trains not shown). The only difference between each paradigm was the interval between potentiating trains of 4, 7 or 10 sec. **B.** The normalized force profiles of the 30 pps trains used to measure potentiation from the 4 sec interval paradigm. Peak force from these trains was plotted in part **A.** (These data are from CF44, with similar results from CF46 for 4 and 7 sec intervals, 10 sec intervals not tested).

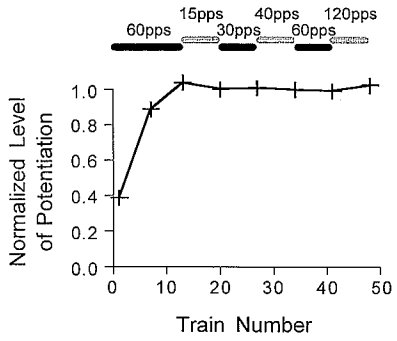

FIG. 4 Normalized level of potentiation during the application of a number of successive stimulus trains. These data were from initial experiments when potentiation was measured from 30 pps 5p trains at 1.0 L_0 (as in Fig. 3). Each data point represents the peak force from one of these trains normalized to the maximal peak force measured during this paradigm. Intervening stimulus trains were at various frequencies from 15 pps to 120 pps. The first 60 pps potentiating trains utilized 10 p trains. The subsequent 15, 30, 40 and 60 pps trains utilized 8 p trains while the final tetanic 120 pps trains used 12 p. All stimulus trains were separated by 7 sec intervals. (These data are from CF50; similar data observed in CF47 and CF68.)

mill walking (Brown *et al.*, 1998). The interval between trains was then varied between 4 and 10 sec while maintaining the same stimulus train (Fig. 5A). We then reverted to 60 pps, 10 p trains at 7 sec intervals for comparison with the previous results. The level of potentiation in this paradigm again plateaued after ~15 trains and never varied by more than 10% under these various conditions. Exponential curves (not shown) fit to the rising phase of potentiation (train # 1–15) from two different experiments produced rate constants of 0.05 and 0.15 sec^{-1}. Force profiles of isometric twitches at L_0 and isometric 43 pps trains at L_0 during the rising phase of potentiation are shown in Figure 5C and 5D. The relative increases in peak force in the potentiated state compared to the unpotentiated state were approximately 400% for the twitch and 65% for the 43 pps train.

At the end of the second paradigm single twitches were applied every 30 sec for 30 min to record the time course of potentiation decay (Fig. 5B). Exponential curves (not shown) were fit to the falling phase of potentiation (from time = 0 to 200 sec). The rate constants from two different experiments were 0.004 and 0.007 sec^{-1} for the falling phase, 20–40× slower than the rising phase.

FL curves for both fused tetanic contractions (120 pps, 12 p) and single twitches in both the unpotentiated and potentiated states are shown in Figure 6. Near-maximal potentiation was obtained with 12 trains of 10 p at 60 pps and 7 sec intervals. For the tetanic FL curves, potentiation was then maintained by the tetanic stimuli themselves (12 p, 120 pps, 7 sec intervals). For the twitch FL curves potentiation was maintained with 8 p trains at 60 pps and 7 sec intervals. Twitch data were collected

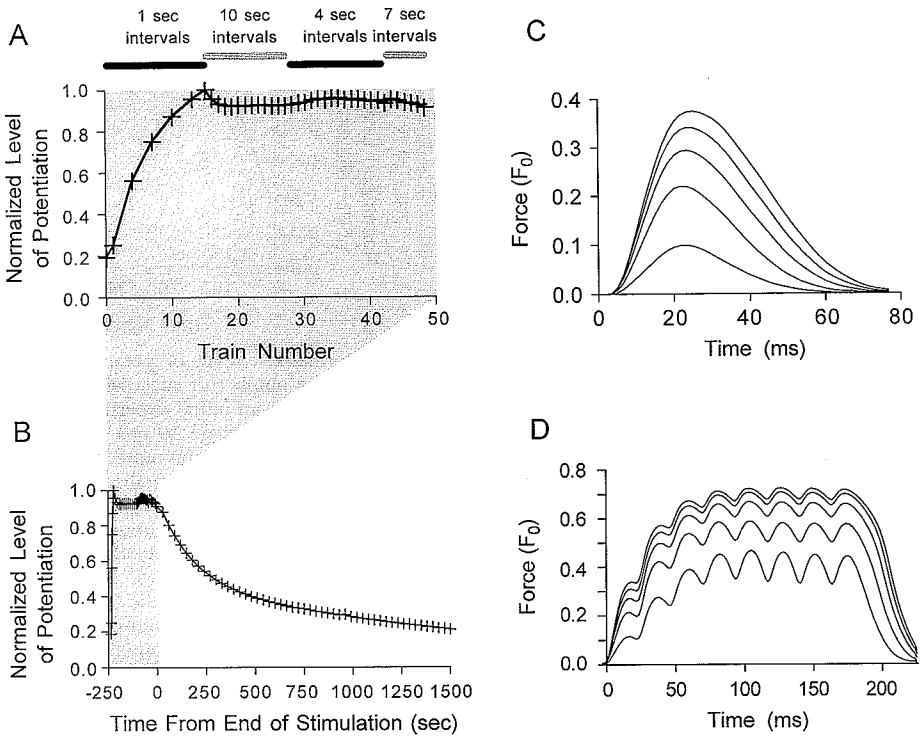

FIG. 5 Normalized level of potentiation during the application of a number of successive stimulus trains. Normalized level of potentiation was defined as the peak force of an isometric twitch at 1.0 L_0, normalized to the maximal level measured during the experiment. Twitches were applied between successive trains. **A.** During the rising phase of potentiation 43 pps, 8p trains were applied at 1 sec intervals, with twitches interposed between only some of the trains. Once potentiation was achieved, the interval between each stimulus train was varied. Stimulus trains 16–27 were also 43 pps, 8p trains but at 10 sec intervals. Stimulus trains 28–42 were again 43 pps, 8p trains but at 4 sec intervals. Stimulus trains 43–48 were 60 pps, 10p trains at 7 sec intervals (same pattern used to potentiate the muscles in Fig. 4). **B.** Same data is in part **A** (shaded region) replotted on a different time axis to also include the decaying phase of potentiation. Time 0 indicates the end of the last stimulus train. **C.** Force profiles of the 2nd–6th isometric twitches at L_0 from part **A.** Force is in units of F_0 (maximal isometric tetanic force in the unpotentiated state). The apparent increase in twitch duration upon potentiation only occurs at lengths near L_0. At longer muscle lengths (*e.g.*, L_0^{tw}) twitch duration actually decreases upon potentiation (data not shown). These changes in twitch duration are consistent with previous studies conducted both at optimal muscle lengths (L_0—Botterman *et al.*, 1986) and at longer muscle lengths (L_0^{tw}—Grange *et al.*, 1995; Vandenboom and Houston, 1996). **D.** Force profiles of the isometric 43 pps trains at L_0 used to potentiate the muscle in part **A.** The five trains were elicited immediately following the five twitches shown in part **C** (*i.e.*, train numbers 2, 5, 8, 11 & 14 in part **A**). Force of these trains increased with the level of potentiation. (These data are from CF55 with similar data observed in CF56.)

during the 7 sec intervals between these potentiating stimuli. Figure 6A shows the actual forces of all the FL curves in units of F_0 (peak unpotentiated, isometric, tetanic force). Peak twitch forces in the potentiated state were higher than the unpotentiated state; surprisingly, peak tetanic force actually decreased slightly in the potentiated state. Subsequent tetanic contractions in the unpotentiated state reached pre-potentiation levels of force, suggesting that some form of short-term fatigue was responsible for the small decrease during potentiation. A summary of the contractile properties of isometric twitches at L_0 for both the unpotentiated and potentiated states is presented in Table 1. Comparative twitch force data from other whole-muscle fast-twitch preparations is presented in Table 2. Because of the large effects of temperature on twitch contractile properties and potentiation (Asmussen and Gaunitz, 1989; Moore *et al.*,

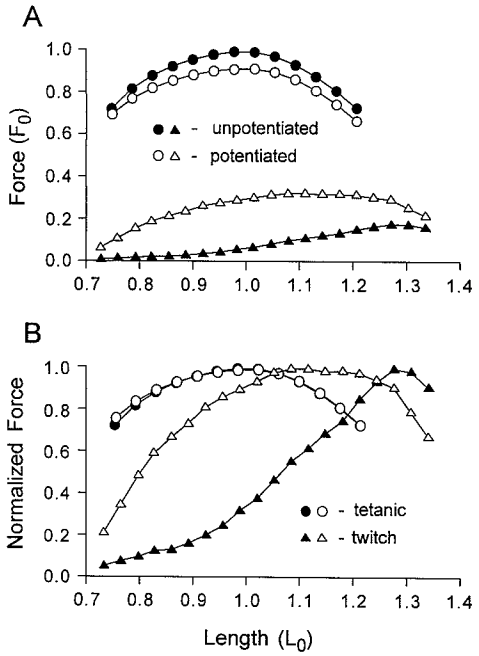

FIG. 6. **A.** Tetanic FL curves (circles; 120 pps, 12 p trains) and twitch FL curves (triangles) collected while CF was in both the unpotentiated (filled symbols) and potentiated states (open symbols). Forces were normalized to the maximum isometric tetanic force in the unpotentiated state (F_0) **B.** The same data as in part **A** are replotted with each FL curve normalized to its maximum force to compare the shapes of the various curves. The tetanic data are from CF56 (similar results in CF57) and the twitch data are from CF58 (similar results observed in CF56, CF57, and CF59, but CF56 only included lengths up to 1.2 L_0, so the peak of the unpotentiated twitch FL curve was not reached.)

1990), only those studies conducted at body temperature were included in Table 2.

To compare the shapes of the various FL curves, Figure 6B shows the twitch and tetanic FL curves in both the unpotentiated and potentiated states normalized to each of their respective maxima. The tetanic FL curves in both states produced similar shapes, while the twitch FL curves were different. The peak of the twitch FL curve shifted from 1.31 ± 0.03 L_0 in the unpotentiated state to 1.15 ± 0.05 L_0 in the potentiated state; this shift of 0.16 ± 0.04 L_0 was significantly different from zero (mean ± S.D.; $n = 3$; $P < 0.01$, Student t-test).

DISCUSSION

Most studies investigating the properties of fast-twitch muscle have employed one of three basic paradigms. One paradigm induces maximal potentiation with a single high-frequency (≥200 pps) long duration (≥1 sec) tetanic train of stimuli (Standaert, 1964; Close and Hoh, 1968) and compares twitches from before and after the conditioning stimulus. A second paradigm produces an effect known as the 'staircase phenomenon' with a single low frequency (≤5 pps), long duration (≥30 sec) train of stimulation (Moore and Stull, 1984; Barnes and Williams, 1990) so that the slow transition from the unpotentiated state to the fully potentiated state can be examined. The third paradigm simply avoids potentiation by employing long passive intervals (≥2 min) between stimulations (Heckman *et al.*, 1992; while previous studies have used 2 min intervals to avoid potentiation, our results [see Fig. 2] suggest that intervals ≥5 min should be used). All of these paradigms are based on the tacit assumption that the unpotentiated state of muscle is a useful base state in which to characterize muscle. This assumption, in turn, leads to models such as shown in Figure 1A in which this base state must be augmented by various additional terms to describe accurately the

TABLE 1. *Isometric twitch contractile properties at 1.0 L_0 for the unpotentiated and potentiated states.*

	Unpotentiated state	Potentiated state	Difference
CT (msec)	21.6 ± 2.1	23.3 ± 1.7	1.7 ± 1.2
½ RT (msec)	13.2 ± 1.6	16.7 ± 2.9	3.5 ± 3.1
PF (F_0)	0.06 ± 0.02	0.30 ± 0.07	0.24 ± 0.05

All values are mean ± standard deviation (n = 11). CT—contraction time. ½ RT—half relaxation time (time from peak force to 50% peak force). PF—peak force normalized to units of F_0 (maximal tetanic isometric force). The difference between the unpotentiated and potentiated states for each of CT, ½ RT and PF was calculated to look for consistent changes with potentiation (see Fig. 5C for an example of the changes seen during potentiation in an isometric twitch at L_0). All three differences (CT, ½ RT and PF) were significantly different from zero ($P < 0.01$, Student's t-test).

TABLE 2. *Comparison of peak isometric twitch forces and the effects of potentiation for different fast-twitch, whole-muscle, mammalian preparations at body temperature (35–38°C).*

	Feline CF	Feline MG	Rat G	Rat EDL	Mouse EDL	Rabbit PL
PF at L_0 (F_0)	0.06 ± 0.02[1]	n/a	n/a	n/a	0.11[9]	n/a
PF at L_0^{tw} (F_0)	0.18 ± 0.05[2]†	0.22[3]	0.17[4], 0.22[5]	0.13[7], 0.14[8]	0.09[10], 0.13[8], 0.23–0.29[11]	0.15[12]
PF*/PF at L_0	5.2 ± 1.5[1]‡	n/a	n/a	n/a	n/a	n/a
PF*/PF at L_0^{tw}	1.6 ± 0.3[2]‡	2.1[3]	1.8[4], 1.5[6]	1.9[7]	1.3[10]	1.6[13]

Values from the current study are mean ± standard deviation. PF and PF*—peak isometric twitch force for the unpotentiated and potentiated states respectively (normalized to units of F_0—maximal tetanic isometric force in the unpotentiated state). L_0—length at which maximal unpotentiated isometric tetanic force occurs. L_0^{tw}—length at which maximal unpotentiated isometric twitch force occurs (L_0^{tw} = 1.31 ± 0.03 L_0 for feline CF). CF—caudofemoralis. MG—medial gastrocnemius. G—gastrocnemius. EDL—extensor digitorum longus. PL—plantaris.

† Significantly different from PF at L_0 ($P < 0.025$; Student's *t*-test).

‡ Significantly greater than 1.0 ($P < 0.025$; Student's *t*-test).

[1] Feline CF data (n = 11) from this study.

[2] Feline CF data (n = 3) from this study.

[3] Burke *et al.* (1976); single motor unit data within a whole-muscle; potentiated state achieved with "several tetani at 80 pps."

[4] Moore and Stull (1984); potentiated state achieved with 10 sec train at 10 pps.

[5] de Haan *et al.* (1986).

[6] MacIntosh and Gardiner (1987) potentiated state achieved with 1 sec train at 200 pps.

[7] Krarup (1981) potentiated state achieved with 50 sec train at 5 pps.

[8] Asmussen and Gaunitz (1989).

[9] Haida *et al.* (1989).

[10] Moore *et al.* (1990); potentiated state achieved with 20 sec train at 5 pps.

[11] Webster and Bressler (1984); range represents different values for different age mice.

[12] Salmons (1992).

[13] Moore *et al.* (1985); potentiated state achieved with 20 sec train at 5 pps.

changes that occur under "special" circumstances such as potentiation. In the following discussion, we argue that the fully potentiated state of muscle is a better base state in which to characterize muscle and from which to build models.

Is potentiation a continuous or bimodal state?

One appeal of the unpotentiated state *vs.* potentiated is that it seems to avoid the question of degree of potentiation. One reasonable explanation for potentiation is that it occurs when myosin regulatory light chains (RLC) are phosphorylated (see Sweeney *et al.,* 1993 for review). Although individual light chains can exist in only one of two states, intermediate levels of potentiation can arise because whole-muscle potentiation depends upon the distribution of these two states. Many previous investigations of potentiation have, in fact, examined intermediate levels of potentiation (Moore and Stull, 1984; Barnes and Williams, 1990; Sweeney *et al.,* 1993) and have shown that the rate of development and steady-state level of potentiation are highly dependent upon stimulus duration and stimulus frequency. Our data (Figs. 3–5) show that potentiation does not develop instantaneously and completely but that it does develop rapidly. Once developed, potentiation persists at a stable plateau for a wide range of patterns of intermittent activation. This stability over a wide range of patterns of activation is distinctly different from what is observed during more 'typical' experimental paradigms (*e.g.,* Moore and Stull, 1984; Barnes and Williams, 1990; Sweeney *et al.,* 1993). We presume that this stable plateau exists because of the large differences in the kinetics for potentiation *vs.* dispotentiation (ratio of time constants is >20:1 as estimated from the data in Fig. 5). It is relatively easy to get muscle into either a maximally potentiated or a completely unpotentiated state but it would be rather difficult to maintain muscle at any stable intermediate state, even though such states are possible. A common example is

the staircase phenomenon where constant low frequency stimulation produces a rising level of potentiation, followed by a plateau at some intermediate level of potentiation (followed later by a decrease in force with the onset of fatigue; Moore and Stull, 1984; Barnes and Williams, 1990). The importance of a bimodal (potentiated/unpotentiated) system from a theoretical viewpoint is that a bimodal system is much easier to control because it is much more predictable.

In which state of potentiation is it easier to conduct experiments on muscle?

For experiments in which it is desirable to sample a reasonably large number of different conditions of activation and/or kinematics, it is much easier to keep the muscle in the fully potentiated state than in a completely unpotentiated state (*e.g.*, see Fig. 2). For stimulation trains of more than a few pulses, it is likely that potentiation is already starting to occur even within the train. Potentiation develops twenty to forty times more rapidly than it decays, making it more difficult to reach and clearly identify a fully unpotentiated state. The data in Figure 3 support this notion because all three protocols produced slightly different initial forces, presumably due to different initial phosphorylation states. In fact, the main impetus for this study was the difficulty of collecting a reasonably complete set of data required to characterize muscle if all of the data had to be obtained under uniformly unpotentiated conditions. Other studies have apparently not encountered this problem, perhaps because they employed a narrower range of activation than used in the present study.

The effects of post-activation potentiation on caudofemoralis

The increase in twitch force following PAP was observed to be highly length dependent in this study (Fig. 6A). At first glance, the unprecedented 420% increase in peak twitch force which we observed at L_0 (Table 1) suggests that CF may be a unique or abnormal preparation. More commonly reported values for increases in twitch force due to PAP are in the 30–110% range for a variety of mammalian fast-twitch preparations at body temperature (Table 2). Most of these experiments, however, were not conducted at L_0; instead they were conducted at the muscle lengths that produced optimal isometric twitch force (L_0^{tw}) for the state of unpotentiation being studied at the time. The increase in twitch force that we observed upon potentiation at L_0^{tw} was only 60%, which lies in the middle of the range of values reported for other muscles (Table 2). A consequence of this length-dependent effect is that the twitch FL curve is shifted to shorter lengths following potentiation. This shift was accompanied by a broadening of the twitch FL curve in our experiments. Close (1972, frog at 20°C) observed a similar length dependence of potentiation and a similar shift to shorter lengths of the twitch FL curve, but observed a narrowing instead of a broadening of the twitch FL curve upon potentiation.

The increase in force that we observed following PAP was also strongly dependent upon stimulus frequency; the increase for stimulus trains at 43 pps was substantially less than that observed for twitches (~65% *vs.* ~400%, both at L_0). Although the effect at different stimulus frequencies was not specifically investigated, our results are consistent with those of Burke *et al.* (1976—feline medial gastrocnemius) who found an increase in force following potentiation at all sub-tetanic frequencies of stimulation, the amount of which became less as stimulus frequency increased. This is in disagreement with the apparent 'threshold' frequency of 20 pps observed by Vandenboom *et al.* (1993—mouse extensor digitorum longus) above which they did not observe an increase in force following potentiation. Our study and that of Burke *et al.* were carried out at 37°C, whereas Vandenboom *et al.* conducted their study at only 25°C. As previously mentioned, temperature has large effects on twitch contractile properties and potentiation (Asmussen and Gaunitz, 1989; Moore *et al.*, 1990), suggesting that the reason for Vandenboom *et al.*'s apparent threshold frequency may be temperature related.

The effects of PAP in CF were similar to previous investigations in one other respect. The rising phase of PAP we observed in CF

occurred at a rate twenty to forty times faster than the decaying phase. Stull and colleagues (Moore and Stull, 1984; Stull *et al.,* 1990) have reported rate constants for light chain phosphorylation and dephosphorylation in rat gastrocnemius of 0.26 sec^{-1} and 0.007 sec^{-1}. These values are similar to our observed rate constants for potentiation/dispotentiation of 0.05–0.15 sec^{-1} and 0.004–0.007 sec^{-1}. The similarity in values is in agreement with the hypothesis that phosphorylation of the myosin light chains is primarily responsible for potentiation. This hypothesis could be tested more directly by measuring levels of myosin light chain phosphorylation in both the unpotentiated and potentiated states.

In what state of potentiation does muscle normally operate?

The frequency, duration and repetition rates of the stimulus trains used in this study were generally within the physiological range of firing frequencies expected during naturally occurring motor behaviors (Bigland and Lippold, 1954; Bellemare *et al.,* 1983; Hoffer *et al.,* 1987), with the exception of the tetanic trains at 120 pps employed for comparison with other studies. Given that a single physiological stimulus train can induce potentiation by itself (Fig. 2) and that multiple stimulus trains at physiological frequencies and intervals result in rapid potentiation (Figs. 3–5), CF muscle fibers used repetitively in a cyclical behaviour such as locomotion could not remain in an unpotentiated state for the duration of the task. Even when starting from a completely unpotentiated state after an extended period of rest (>10 min), the unpotentiated state would be expected to last only for the first few cycles of locomotion. Interestingly, animals and humans often elect to use various "warm up" movements before they start a new task after resting, especially if accurate performance is desired. It seems possible that these preparatory movements may serve, at least in part, to potentiate the contractile mechanism of any fast-twitch muscle fibers that will be used in the task, thereby assuring a stable and predictable level of force output.

What states of muscle function should be used as the basis for muscle models?

The traditional approach to modeling is to derive the simplest possible set of independent functions that each describe some well-known state of muscle. Additional terms are then gradually added to deal with complexities and interdependencies between functions that appear to arise when other states of muscle are studied. Mathematics itself provides no guidance about which of several possible states to use as the base; knowledge of structure and function underlying those functions, however, can be most instructive.

Consider the effects that potentiation has on the twitch FL curve (Fig. 6). If we used history as our guide to help design our model, we would begin with the unpotentiated state as the base state. This would require a complex term added to F_{ACT} to account for the differences between the tetanic and twitch FL curves in the unpotentiated state, and then a second complex term added to F_{ACT} to account for the differences between the unpotentiated state and the potentiated state (Fig. 6). Earlier we argued that the normal operating state of fast-twitch muscle is, in fact, the potentiated state. We therefore suggest that in designing our mathematical model of muscle, we should begin with the potentiated state as our base state. This would then provide us with a simpler model requiring only one corrective term to account for small differences observed in the shapes of the twitch and tetanic FL curves in the potentiated state.

ACKNOWLEDGMENTS

The authors would like to thank Janet Creasy, David Kim and Kan Singh for technical assistance with the experiments. This research was funded by the Medical Research Council of Canada.

REFERENCES

Asmussen, G. and U. Gaunitz. 1989. Temperature effects on isometric contractions of slow and fast twitch muscles of various rodents—dependence of fiber type compositions: A comparative study. Biomed. Biochim. Acta 48(5):S536–S541.

Barnes, W. S. and J. H. Williams. 1990. Staircase potentiation in isolated frog skeletal muscle: Power

spectral analysis of the evoked compound muscle action potential. Comp. Biochem. Physiol. 96A: 387–394.

Bellemare, F., J. J. Woods, R. Johansson, and B. R. Bigland-Ritchie. 1983. Motor-unit discharge rates in maximal voluntary contractions of three human muscles. J. Neurophysiol. 50(6):1380–1392.

Bigland, B. and O. C. J. Lippold. 1954. Motor unit activity in the voluntary contraction of human muscle. J. Physiol. 125:322–335.

Botterman, B. R., G. A. Iwamoto, and W. J. Gonyea. 1986. Gradation of isometric tension by different activation rates in motor units of cat flexor carpi radialis muscle. J. Neurophysiol. 56(2):494–506.

Brown, I. E., T. L. Liinamaa, and G. E. Loeb. 1996*a*. Relationships between range of motion, L_0 and passive force in five strap-like muscles of the feline hindlimb. J. Morphol. 230:69–77.

Brown, I. E., T. Satoda, F. J. R. Richmond, and G. E. Loeb. (1998). Feline caudofemoralis muscle: Muscle fiber properties, architecture, and motor innervation. Exp. Brain Res. 121:76–91.

Brown, I. E., S. H. Scott, and G. E. Loeb. 1996*b*. Mechanics of feline soleus: II. Design and validation of a mathematical model. J. Muscle Res. Cell Motil. 17:219–232.

Brown, I. E. and G. E. Loeb. (1998). A reductionist approach to creating and using neuromusculoskeletal models. *In* J. M. Winters and P. E. Crago (eds.), *Biomechanics and neural control of movement,* Ch. 3.3, Springer-Verlag, New York.

Burke, R. E., P. Rudomin, and F. E. I. Zajac. 1976. The effect of activation history on tension production by individual muscle units. Brain Res. 109:515–529.

Close, R. I. 1972. The relations between sarcomere length and characteristics of isometric twitch contractions of frog sartorius muscle. J. Physiol. 220(3):745–762.

Close, R. and J. F. Y. Hoh. 1968. The after-effects of repetitive stimulation on the isometric twitch contraction of rat fast skeletal muscle. J. Physiol. 197: 461–477.

de Haan, A., J. de Jong, J. E. van Doorn, P. A. Huijing, R. D. Woittiez, and H. G. Westra. 1986. Muscle economy of isometric contractions as a function of stimulation time and relative muscle length. Pflugers Arch. 407(4):445–450.

Grange, R. W., C. R. Cory, R. Vandenboom, and M. E. Houston. 1995. Myosin phosphorylation augments force-displacement and force-velocity relationships of mouse fast muscle. Am. J. Physiol. 269(3):C713–C724.

Haida, N., W. M. Fowler, Jr., R. T. Abresch, D. B. Larson, R. B. Sharman, R. G. Taylor, and R. K. Entrikin. 1989. Effect of hind-limb suspension on young and adult skeletal muscle. I. Normal mice. Exp. Neurol. 103(1):68–76.

Heckman, C. J., J. L. F. Weytjens, and G. E. Loeb. 1992. Effect of velocity and mechanical history on the forces of motor units in the cat medial gastrocnemius muscle. J. Neurophysiol. 68:1503–1515.

Hoffer, J. A., N. Sugano, G. E. Loeb, W. B. Marks, M. J. O'Donovan, and C. A. Pratt. 1987. Cat hindlimb motoneurons during locomotion: II. Normal activity patterns. J. Neurophysiol. 57:530–553.

Krarup, C. 1981. Enhancement and diminution of mechanical tension evoked by staircase and by tetanus in rat muscle. J. Physiol. 311:355–372.

Loeb, G. E., J. He, and W. S. Levine. 1994. The relationship between reflexive and intrinsic control of limb trajectories. Can. Soc. for Biomech. 7g–7h.

MacIntosh, B. R. and P. F. Gardiner. 1987. Posttetanic potentiation and skeletal muscle fatigue: Interactions with caffeine. Can. J. Physiol. Pharmacol. 65(2):260–268.

Manning, D. R. and J. T. Scull. 1982. Myosin light chain phosphorylation-dephosphorylation in mammalian skeletal muscle. Am. J. Physiol. 242: c234–c241.

Moore, R. L., M. E. Houston, G. A. Iwamoto, and J. T. Scull. 1985. Phosphorylation of rabbit skeletal muscle myosin *in situ.* J. Cell Physiol. 125:301–305.

Moore, R. L., B. M. Palmer, S. L. Williams, H. Tanabe, R. W. Grange, and M. E. Houston. 1990. Effect of temperature on myosin phosphorylation in mouse skeletal muscle. Am. J. Physiol. 259(3): C432–C438.

Moore, R. L. and A. Persechini. 1990. Length-dependence of isometric twitch tension potentiation and myosin phosphorylation in mouse skeletal muscle. J. Cell Physiol. 143:257–262.

Moore, R. L. and J. T. Scull. 1984. Myosin light chain phosphorylation in fast and slow skeletal muscle *in situ.* Am. J. Physiol. 247:c462–c471.

Rack, P. M. H. and D. R. Westbury. 1969. The effects of length and stimulus rate on tension in the isometric cat soleus muscle. J. Physiol. 204:443–460.

Salmons, S. 1992. Myotrophic effects of an anabolic steroid in rabbit limb muscles. Muscle Nerve 15(7):806–812.

Scott, S. H., I. E. Brown, and G. E. Loeb. 1996. Mechanics of feline soleus: I. Effect of fascicle length and velocity on force output. J. Muscle Res. Cell Motil. 17:205–218.

Shue, G., P. E. Crago, and H. J. Chizeck. 1995. Muscle-joint models incorporating activation dynamics, moment-angle, and moment-velocity properties. IEEE Trans. Biomed. Eng. 42(2):212–222.

Standaert, F. G. 1964. The mechanisms of post-tetanic potentiation in cat soleus and gastrocnemius muscles. J. Gen. Physiol. 47:987–1001.

Stephenson, D. G. and I. R. Wendt. 1984. Length dependence of changes in sarcoplasmic calcium concentration and myofibrillar calcium sensitivity in striated muscle fibres. J. Muscle Res & Cell Motility 5:243–272.

Stull, J. T., B. F. Bowman, P. J. Gallagher, B. P. Herring, L. C. Hsu, K. E. Kamm, Y. Kubota, S. A. Leachman, H. L. Sweeney, and M. G. Tansey. 1990. Myosin phosphorylation in smooth and skeletal muscles: Regulation and function. [Review] [69 refs]. Prog. Clin. Biol. Res. 327:107–126.

Sweeney, H. L., B. F. Bowman, and J. T. Stull. 1993.

Myosin light chain phosphorylation in vertebrate striated muscle: Regulation and function. Am. J. Physiol. 264:c1085–c1095.

Vandenboom, R., R. W. Grange, and M. E. Houston. 1993. Threshold for force potentiation associated with skeletal myosin phosphorylation. Am. J. Physiol. 265:C1456–C1462.

Vandenboom, R. and M. E. Houston. 1996. Phosphorylation of myosin and twitch potentiation in fatigued skeletal muscle. Can. J. Physiol. Pharmacol. 74(12):1315–1321.

Webster, D. M. and B. H. Bressler. 1985. Changes in isometric contractile properties of extensor digitorum longus and soleus muscles of C57BL/6J mice following denervation. Can. J. Physiol. Pharmacol. 63(6):681–686.

Zajac, F. E. 1989. Muscle and tendon: Properties, models, scaling and application to biomechanics and motor control. Crit. Rev. Biomed. Engng. 17(4): 359–411.

Corresponding Editor: Todd Gleason